

Rotational Spectrum of the Hydrogen-Bonded Dimer CH₃CN...HCl

A. C. Legon,*

Department of Chemistry, University of Exeter, Exeter EX4 4QD, United Kingdom

D. J. Millen,* and H. M. North

Department of Chemistry, Christopher Ingold Laboratories, University College London, London WC1H 0AJ, United Kingdom (Received: April 1, 1987)

Chlorine nuclear quadrupole hyperfine structure has been resolved and analyzed in the spectrum of three isotopic species, CH₃C¹⁵N...H³⁵Cl, CH₃C¹⁵N...H³⁷Cl, and CH₃C¹⁵N...D³⁵Cl, of the methyl cyanide-hydrogen chloride hydrogen-bonded dimer. The determined spectroscopic constants are $B_0 = 1\,100.726\,75$ (8) MHz, $D_J = 0.554$ (1) kHz, $D_{JK} = 64.05$ (5) kHz, and $eqQ = -52.45$ (2) MHz for CH₃C¹⁵N...H³⁵Cl. These spectroscopic constants have been interpreted to give $r(\text{N...Cl})$ and k_σ , the values of which are 3.301 (4) Å and 10.68 (2) N m⁻¹, respectively, for the species CH₃C¹⁵N...H³⁵Cl. The corresponding quantities are also presented for the species CH₃C¹⁵N...H³⁷Cl and CH₃C¹⁵N...D³⁵Cl.

Introduction

We have recently been systematically investigating the rotational spectra of a series of hydrogen-bonded dimers with the aim of drawing general conclusions about the nature of the hydrogen bonds. The current state of the development of these conclusions has been reviewed recently in several articles.¹⁻³ The properties about which conclusions have been established include angular geometries, the lengthening of the HF bond on formation of B...HF, and the strength of intermolecular binding as measured by the intermolecular stretching force constant, k_σ . The dimers HCN...HX and CH₃CN...HX, where X = F, Cl, Br, and CN, have featured strongly in making the generalizations,¹⁻³ but so far the detailed rotational spectroscopy of CH₃CN...HCl and CH₃CN...HBr has not been published. In the present article we present a detailed analysis of the spectrum of CH₃CN...HCl and determine the properties that are important for the generalizations.¹⁻³ The more difficult case of CH₃CN...HBr will be discussed elsewhere.⁴

Experimental Section

The rotational spectrum of each of three isotopic species, CH₃C¹⁵N...H³⁵Cl, CH₃C¹⁵N...H³⁷Cl, and CH₃C¹⁵N...D³⁵Cl, of the dimer CH₃CN...HCl was observed and measured by using the pulsed-nozzle, Fourier-transform, microwave spectrometer which has been described elsewhere.⁵ In searching for the transitions initially, we used a gas mixture of the most abundant isotopic species consisting of about 2% of each monomer diluted to a total pressure of 2 atm with argon. Once the rotational spectrum of the dimer had been identified, the normal isotopic species of methyl cyanide was replaced by the ¹⁵N species in order to simplify the rotational spectrum. Unlike the ¹⁴N nucleus, that of ¹⁵N has a spin of $I = 1/2$ and therefore it does not possess a quadrupole moment. The complicated structure of rotational transitions in, for example, CH₃C¹⁴N...H³⁵Cl caused by the presence of the two quadrupolar nuclei ¹⁴N and ³⁵Cl is thus avoided.

Methyl cyanide was supplied by BDH Chemicals PLC and hydrogen chloride by Argo. The ¹⁵N species of methyl cyanide was prepared by the dehydration of [¹⁵N]ammonium acetate which was supplied by Amersham International PLC.

In addition to the rotational spectrum of CH₃C¹⁵N...HCl the spectrum of the complex CH₃C¹⁵N...D³⁵Cl was observed and measured. Deuterium chloride was prepared by dropping a mixture of DCl in D₂O on to excess phosphorus pentoxide at

reduced pressure. The vapor evolved was condensed at liquid nitrogen temperatures. Before introducing this sample of DCl into the mixing chamber of the spectrometer, we flushed the chamber with D₂O to minimize any exchange of deuterium on the walls.

Results

Rotational Spectrum and Spectroscopic Constants. The rotational spectra of the species CH₃C¹⁵N...H(D)³⁵Cl and CH₃C¹⁵N...H³⁷Cl have been observed and measured in the frequency range 8-16 GHz. Each $J + 1 \leftarrow J$ ground-state rotational transition of these symmetric rotor molecules in principle consists of several closely spaced K components in addition to a number of quadrupole components that are concomitants of the presence of the Cl ($I = 3/2$) nucleus. The very low effective temperature of the gas mixture during its supersonic expansion into the cavity of the spectrometer ensures that only the lowest K states are sufficiently populated to be observed. The structure of a representative transition is illustrated in Figure 1 for the species CH₃C¹⁵N...H³⁷Cl. The interpenetration of the hyperfine components of different K is clearly seen.

For each of the three isotopic species, only the $\Delta F = +1$ components with $K = 0$ and $K = 1$ were intense enough to be observed. Figure 2 shows one quadrupole component each of the $K = 0$ and the $K = 1$ components of the $J = 5 \leftarrow 4$ transition for the species CH₃C¹⁵N...H³⁷Cl, both of which happen to fall within the bandwidth of the spectrometer when tuned to the indicated frequency. Three quadrupole components of the same rotational transition of the isotope species CH₃C¹⁵N...D³⁵Cl are displayed in Figure 3. Observed frequencies are collected in Tables I, II, and III for the species CH₃C¹⁵N...H³⁵Cl, CH₃C¹⁵N...H³⁷Cl, and CH₃C¹⁵N...D³⁵Cl, respectively. These were fitted by a standard nonlinear, least-squares procedure that employed complete diagonalization of the Hamiltonian matrix constructed in the coupled basis $\mathbf{J} + \mathbf{I} = \mathbf{F}$. The form of the Hamiltonian is

$$H = H_R + H_Q \quad (1)$$

where

$$H_Q = -\frac{1}{6}Q_e \nabla E \quad (2)$$

accounts for the Cl nuclear quadrupole interaction with the electric field gradient⁶ and where H_R is the familiar semirigid rotor Hamiltonian appropriate to a symmetric-top molecule. The matrix elements of H_Q in the coupled basis are well-known.⁶ The differences between the observed frequencies and those calculated in the final cycle of the fitting procedure are included, as appropriate, in Tables I-III. The spectroscopic constants B_0 , D_J ,

(1) Legon, A. C.; Millen, D. J. *Chem. Rev.* **1986**, *86*, 635.

(2) Legon, A. C.; Millen, D. J. *Acc. Chem. Res.* **1987**, *20*, 39.

(3) Legon, A. C.; Millen, D. J. *J. Am. Chem. Soc.* **1987**, *109*, 356.

(4) Legon, A. C.; Millen, D. J.; North, H. M., to be published.

(5) Legon, A. C.; Willoughby, L. C. *Chem. Phys.* **1983**, *74*, 127.

(6) Townes, C. H.; Schawlow, A. L. *Microwave Spectroscopy*; McGraw-Hill: New York, 1955.

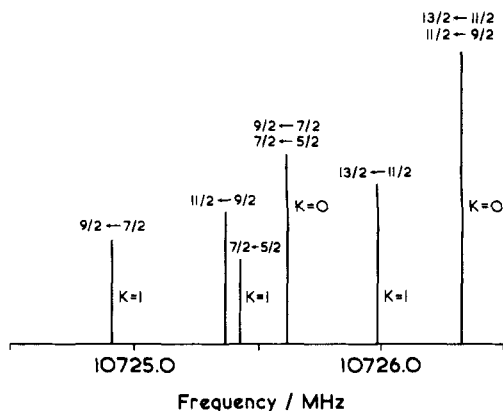


Figure 1. Stick diagram illustrating the interpenetration of the ³⁷Cl nuclear quadrupole components in the $K = 0$ and $K = 1$ components of the $J = 5 \leftarrow 4$ transition of $\text{CH}_3\text{C}^{15}\text{N}\cdots\text{H}^{37}\text{Cl}$.

TABLE I: Observed and Calculated Rotational Transition Frequencies of $\text{CH}_3\text{C}^{15}\text{N}\cdots\text{H}^{35}\text{Cl}$

J'	F'	J''	F''	K	$\nu_{\text{obsd}}/\text{MHz}$	$(\nu_{\text{obsd}} - \nu_{\text{calcd}})/\text{kHz}$
4	11/2	3	9/2	0	8806.0701	-0.9
	9/2		7/2	0	8806.0701	0.1
	7/2		5/2	0	8804.5448	1.4
	5/2		3/2	0	8804.5448	-3.1
4	7/2	3	5/2	1	8803.9405	0.0
	9/2		7/2	1	8804.6207	-0.5
	5/2		3/2	1	8805.2466	-1.5
	11/2		9/2	1	8805.9362	-0.7
5	13/2	4	11/2	0	11007.2665	0.0
	11/2		9/2	0	11007.2665	0.6
	9/2		7/2	0	11006.3658	2.4
	7/2		5/2	0	11006.3658	0.5
5	9/2	4	7/2	1	11005.5996	0.2
	11/2		9/2	1	11006.1801	0.6
	7/2		5/2	1	11006.2526	-1.1
	13/2		11/2	1	11006.8370	-0.3
6	15/2	5	13/2	0	13208.4449	0.3
	13/2		11/2	0	13208.4449	0.7
	11/2		9/2	0	13207.8441	0.9
	9/2		7/2	0	13207.8441	0.0
6	11/2	5	9/2	1	13206.9787	0.0
	9/2		7/2	1	13207.3527	-0.2
	13/2		11/2	1	13207.4299	-0.1
	15/2		13/2	1	13207.8085	2.6
7	17/2	6	15/2	0	15409.5680	-0.8
	15/2		13/2	0	15409.5680	-0.6
	13/2		11/2	0	15409.1374	-0.4
	11/2		9/2	0	15409.1374	-0.9

D_{JK} , and eQq thereby determined are recorded in Table IV for each isotopic species.

Interpretation of Nuclear Quadrupole Coupling Constants. If the electric field gradient at the Cl nucleus is assumed effectively unchanged on dimer formation, the observed Cl nuclear quadrupole coupling constants eQq are related to the corresponding eQq_0 for the free HCl molecule⁷ by

$$eQq = \frac{1}{2}eQq_0(3 \cos^2 \theta - 1) \quad (3)$$

where θ is the instantaneous angle between the HCl axis and the molecular a axis (see Figure 4) and the average is over the zero-point motion. Equation 3 can then be used to obtain the operationally defined angles

$$\theta_{\text{av}} = \cos^{-1} \langle \cos^2 \theta \rangle^{1/2} \quad (4)$$

the values of which are given in Table V.

Molecular Geometry. In a first analysis, the dimer $\text{CH}_3\text{C}-\text{N}\cdots\text{HCl}$ was assumed to have a linear equilibrium arrangement

TABLE II: Observed and Calculated Rotational Transition Frequencies of $\text{CH}_3\text{C}^{15}\text{N}\cdots\text{H}^{37}\text{Cl}$

J'	F'	J''	F''	K	$\nu_{\text{obsd}}/\text{MHz}$	$(\nu_{\text{obsd}} - \nu_{\text{calcd}})/\text{kHz}$
4	11/2	3	9/2	0	8581.2805	0.1
	9/2		7/2	0	8581.2805	0.7
	7/2		5/2	0	8580.0772	1.0
	5/2		3/2	0	8580.0772	-1.8
4	7/2	3	5/2	1	8579.5138	-0.6
	9/2		7/2	1	8580.0543	2.7
	5/2		3/2	1	8580.5438	-2.8
	11/2		9/2	1	8581.0890	0.1
5	13/2	4	11/2	0	10726.3300	-0.1
	11/2		9/2	0	10726.3300	0.3
	9/2		7/2	0	10725.6190	0.9
	7/2		5/2	0	10725.6190	-0.3
5	9/2	4	7/2	1	10724.9085	0.3
	11/2		9/2	1	10725.3664	0.6
	7/2		5/2	1	10725.4238	-0.8
	13/2		11/2	1	10725.8841	-0.3
6	15/2	5	13/2	0	12871.3547	-0.3
	13/2		11/2	0	12871.3547	0.0
	11/2		9/2	0	12870.8809	0.1
	9/2		7/2	0	12870.8809	-0.6
6	11/2	5	9/2	1	12870.0720	1.6
	9/2		7/2	1	12870.3637	-1.9
	13/2		11/2	1	12870.4250	-1.4
	15/2		13/2	1	12870.7249	2.2

TABLE III: Observed and Calculated Rotational Transition Frequencies of $\text{CH}_3\text{C}^{15}\text{N}\cdots\text{D}^{35}\text{Cl}$

J'	F'	J''	F''	K	$\nu_{\text{obsd}}/\text{MHz}$	$(\nu_{\text{obsd}} - \nu_{\text{calcd}})/\text{kHz}$
4	11/2	3	9/2	0	8784.8529	0.9
	9/2		7/2	0	8784.8529	1.9
	7/2		5/2	0	8783.2877	0.8
	5/2		3/2	0	8783.2877	-3.9
4	7/2	3	5/2	1	8782.7028	-0.1
	9/2		7/2	1	8783.4008	0.5
	5/2		3/2	1	8784.0398	-2.5
	11/2		9/2	1	8784.7504	2.2
5	13/2	4	11/2	0	10980.7409	-3.4
	11/2		9/2	0	10980.7409	-2.8
	9/2		7/2	0	10979.8233	4.2
	7/2		5/2	0	10979.8233	2.2
5	9/2	4	7/2	1	10979.0790	0.6
	11/2		9/2	1	10979.6731	0.4
	7/2		5/2	1	10979.7474	-1.3
	13/2		11/2	1	10980.3468	0.2

TABLE IV: Spectroscopic Constants for the Vibrational Ground State of $\text{CH}_3\text{C}^{15}\text{N}\cdots\text{H}(\text{D})\text{Cl}$

spectroscopic constant	$\text{CH}_3\text{C}^{15}\text{N}\cdots\text{H}^{35}\text{Cl}$	$\text{CH}_3\text{C}^{15}\text{N}\cdots\text{H}^{37}\text{Cl}$	$\text{CH}_3\text{C}^{15}\text{N}\cdots\text{D}^{35}\text{Cl}$
B_0/MHz	1100.72675 (8)	1072.6376 (1)	1098.0719 (4)
D_J/kHz	0.554 (1)	0.528 (2)	0.515 (8)
D_{JK}/kHz	64.05 (5)	61.23 (5)	61.4 (1)
eQq/MHz	-52.45 (2)	-41.38 (3)	-53.73 (5)

TABLE V: Geometries for $\text{CH}_3\text{C}^{15}\text{N}\cdots\text{H}(\text{D})\text{Cl}$

species	$\theta_{\text{av}}/\text{deg}$	$\langle r_{\text{cm}}^{-2} \rangle^{1/2}/\text{\AA}$	$r(\text{N}\cdots\text{Cl})/\text{\AA}$	
			I ^a	II ^b
$\text{CH}_3\text{C}^{15}\text{N}\cdots\text{H}^{35}\text{Cl}$	22.75 (2)	4.5505 (1)	3.29076 (1)	3.3011 (35)
$\text{CH}_3\text{C}^{15}\text{N}\cdots\text{H}^{37}\text{Cl}$	22.71 (3)	4.5522 (8)	3.29070 (1)	3.3028 (35)
$\text{CH}_3\text{C}^{15}\text{N}\cdots\text{D}^{35}\text{Cl}$	21.57 (5)	4.5152 (8)	3.28885 (1)	3.2942 (34)

^a Calculated assuming C_{3v} rigid arrangement $\text{CH}_3\text{CN}\cdots\text{HCl}$ with unperturbed r_0 monomer geometries (see text). ^b Calculated using a model that allows for the zero-point oscillations of the subunits (see text).

$\text{CCN}\cdots\text{HCl}$ of the nuclei and the subunit geometries were assumed unperturbed by dimer formation. The distance between the two subunits was then varied for each isotopic species until the observed

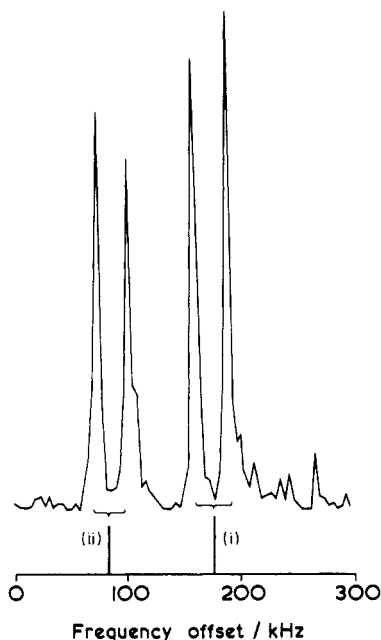


Figure 2. Frequency-domain spectrum of $\text{CH}_3\text{C}^{15}\text{N}\cdots\text{H}^{37}\text{Cl}$ showing two ^{37}Cl nuclear quadrupole components in the $J = 5 \leftarrow 4$ transition. (i) corresponds to the $(9/2 \leftarrow 7/2, 7/2 \leftarrow 5/2)$ unresolved pair of components of the $K = 0$ transition, and (ii) corresponds to the $(13/2 \leftarrow 11/2)$ component of the $K = 1$ transition. Each transition is doubled by an instrumental effect. Frequencies are offset from 10 725.8000 MHz.

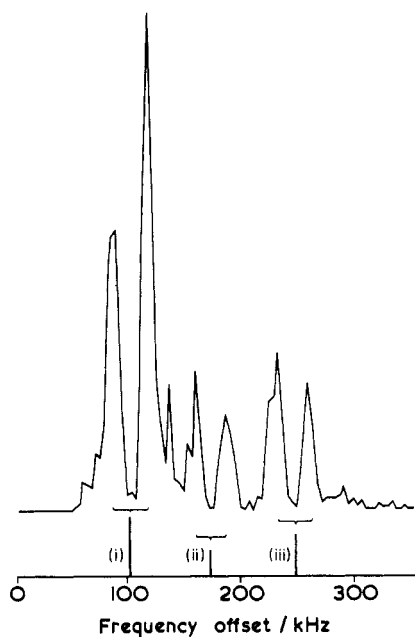


Figure 3. Frequency-domain spectrum of $\text{CH}_3\text{C}^{15}\text{N}\cdots\text{D}^{35}\text{Cl}$ showing three ^{35}Cl nuclear quadrupole components in the $J = 5 \leftarrow 4$ transition. (i) corresponds to the $(9/2 \leftarrow 7/2, 7/2 \leftarrow 5/2)$ unresolved pair of components of the $K = 0$ transition, (ii) corresponds to the $7/2 \leftarrow 5/2$ component of the $K = 1$ transition, and (iii) corresponds to the $11/2 \leftarrow 9/2$ component of the $K = 1$ transition. Frequencies are offset from 10 979.9250 MHz.

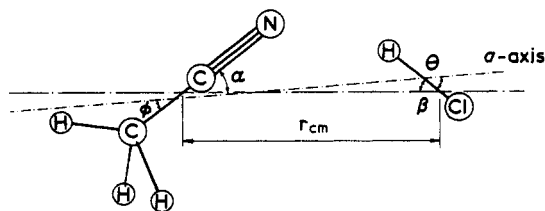


Figure 4. Quantities r_{cm} , α , β , ϕ , and θ used in the discussion of the geometry of $\text{CH}_3\text{C}^{15}\text{N}\cdots\text{HCl}$.

TABLE VI: Intermolecular Stretching Force Constants and Wavenumbers for the Dimer $\text{CH}_3\text{CN}\cdots\text{HCl}$

species	$k_\sigma/\text{N m}^{-1}$	$\bar{\nu}_\sigma/\text{cm}^{-1}$
$\text{CH}_3\text{C}^{15}\text{N}\cdots\text{H}^{35}\text{Cl}$	10.68 (2)	96.7 (9)
$\text{CH}_3\text{C}^{15}\text{N}\cdots\text{H}^{37}\text{Cl}$	10.72 (5)	95.5 (2)
$\text{CH}_3\text{C}^{15}\text{N}\cdots\text{D}^{35}\text{Cl}$	11.54 (2)	99.8 (8)

TABLE VII: Comparison of Molecular Properties in the Series of Dimers $\text{CH}_3\text{CN}\cdots\text{HX}$ and $\text{HCN}\cdots\text{HX}$

species	$r(\text{N}\cdots\text{H})/\text{\AA}$	$k_\sigma/\text{N m}^{-1}$
$\text{CH}_3\text{CN}\cdots\text{HF}$	1.834 ^a	20.1 ^a
$\text{CH}_3\text{CN}\cdots\text{HCl}$	2.007 ^b	10.7 ^b
$\text{CH}_3\text{CN}\cdots\text{HBr}$	2.069 ^c	
$\text{CH}_3\text{CN}\cdots\text{HCN}$	2.150 ^d	9.8 ^d
$\text{HCN}\cdots\text{HF}$	1.879 ^e	18.3 ^e
$\text{HCN}\cdots\text{HCl}$	2.121 ^f	9.2 ^e
$\text{HCN}\cdots\text{HBr}$	2.186 ^h	7.3 ^e
$\text{HCN}\cdots\text{HCN}$	2.224 ⁱ	8.1 ⁱ

^aReference 12. ^bThis work. ^cReference 4. ^dReference 14. ^eReference 15. ^fReference 16. ^gReference 17. ^hReference 18. ⁱReference 19.

value of the rotational constant B_0 was reproduced. The geometries of free methyl cyanide and HCl were taken to be the zero-point versions given in ref 8 or implied by the B_0 value in ref 9, respectively. The results of this procedure are recorded in Table V.

A commonly used alternative¹⁰ for finding the distance between the subunits in the dimer relies on the expression

$$I_b \approx \langle I_{bb} \rangle = \mu r_{\text{cm}}^2 + \frac{1}{2} I_b^{\text{CH}_3\text{CN}} \langle 1 + \cos^2 \alpha \rangle + \frac{1}{2} I_a^{\text{CH}_3\text{CN}} \langle \sin^2 \alpha \rangle + \frac{1}{2} I_b^{\text{HCl}} \langle 1 + \cos^2 \beta \rangle \quad (5)$$

where for present purposes the I_b values are operationally defined as $I_b = h/8\pi^2 B_0$ in terms of the zero-point rotational constants of the components^{9,11} and where α , β , and r_{cm} are as defined in Figure 4. We note that strictly α and β are the instantaneous angles made by the CH_3CN and HCl symmetry axes, respectively, with the line r_{cm} and differ slightly from ϕ and θ . The treatment used here assumes $\phi_{\text{av}} \approx \alpha_{\text{av}}$ and $\theta_{\text{av}} \approx \beta_{\text{av}}$ where the average is of the type defined in eq 4. The differences are negligible. The value used for ϕ_{av} is that determined¹² for CH_3CN in $\text{CH}_3\text{C}\cdots\text{N}\cdots\text{HF}$, namely, $7.0 (1.2)^\circ$, while $\theta_{\text{av}} = 22.75 (2)^\circ$ is taken from Table V. Values of $\langle r_{\text{cm}}^2 \rangle^{1/2}$ can then be determined, with the result included in Table V. Finally, we also give in Table V the distance $r(\text{N}\cdots\text{Cl})$ calculated from

$$r(\text{N}\cdots\text{Cl}) = \langle r_{\text{cm}}^2 \rangle^{1/2} - Z_{\text{N}} \cos \phi_{\text{av}} + Z_{\text{Cl}} \cos \theta_{\text{av}} \quad (6)$$

in which Z_{N} and Z_{Cl} are the distances of the N and Cl nuclei from the centers of mass of CH_3CN and HCl , respectively, and which can be calculated from the monomer geometries referred to above.

Intermolecular Stretching Force Constant. The intermolecular stretching force constant k_σ of $\text{CH}_3\text{CN}\cdots\text{HCl}$ is available from the centrifugal distortion constant D_J with the aid of the expression¹³

$$k_\sigma = (16\pi^2 B_0^3 \mu / D_J) \left\{ 1 - \frac{B_0}{B^{\text{CH}_3\text{CN}}} - \frac{B_0}{B^{\text{HCl}}} \right\} \quad (7)$$

the derivation of which treats the subunits as rigid bodies. The necessary D_J and B_0 values are in Table IV while the B values of the components were taken from ref 8 and 9. The resulting k_σ and the $\bar{\nu}_\sigma$ implied by

(8) Thomas, L. F.; Sherrard, E. I.; Sheridan, J. *Trans. Faraday Soc.* **1955**, *51*, 619.

(9) DeLucia, F. C.; Helminger, P.; Gordy, W. *Phys. Rev. A* **1971**, *3*, 1849.

(10) Legon, A. C.; Willoughby, L. C. *Chem. Phys.* **1984**, *85*, 443.

(11) Demaison, J.; Dubrulle, A.; Boucher, D.; Burie, J.; Tjypke, V. *J. Mol. Spectrosc.* **1979**, *76*, 1.

(12) Cope, P.; Millen, D. J.; Willoughby, L. C.; Legon, A. C. *J. Chem. Soc., Faraday Trans. 2* **1986**, *82*, 1197.

(13) Millen, D. J. *Can. J. Chem.* **1985**, *63*, 1477.

$$\bar{\nu}_\sigma = (1/2\pi c)(k_\sigma/\mu)^{1/2} \quad (8)$$

are recorded in Table VI.

Conclusions

The results presented in the present article allow us to compare the lengths and strengths of hydrogen bonds within and among the series HCN...HX and CH₃CN...HX where X = F, Cl, CN, and Br. The hydrogen bond lengths $r(\text{N}\cdots\text{H})$ have been calculated from the measured $r(\text{N}\cdots\text{X})$ ^{12,15,16,18,19} under the assumption that the HX bond length r_0 survives dimer formation. The results are collected in Table VII, in which we also include the k_σ for these series.^{12,14,15,17,19}

(14) Legon, A. C.; Howard, N. W. *J. Chem. Soc., Faraday Trans. 2* **1987**, 83, 991.

(15) Legon, A. C.; Millen, D. J.; Willoughby, L. C. *Proc. R. Soc. London, A* **1985**, 401, 327.

(16) Legon, A. C.; Campbell, E. J.; Flygare, W. H. *J. Chem. Phys.* **1982**, 76, 2267.

(17) See: Goodwin, E. J.; Legon, A. C. *J. Chem. Phys.* **1986**, 84, 1988.

The dimers CH₃CN...HX are seen (Table VII) to exhibit stronger and shorter hydrogen bonds than their HCN...HX counterparts. These relationships are readily understood in terms of the familiar inductive effect of the CH₃ group relative to the H atom. In each series RCN...HX, the strength of the hydrogen bond (as measured by k_σ) increases in the order Br, CN, Cl, F, in accord with the increasing electrophilicities³ of the HX molecules of the same series.

Acknowledgment. We thank the S.E.R.C. for grants in support of our work on hydrogen bonding and for a research studentship (H.M.N.). We also thank Mr. C. J. Cooksey of U.C.L. for preparing the sample of CH₃C¹⁵N.

Registry No. CH₃C¹⁵N, 14149-39-4; H³⁵Cl, 13779-43-6; H³⁷Cl, 13760-18-4; D³⁵Cl, 14986-26-6.

(18) Campbell, E. J.; Legon, A. C.; Flygare, W. H. *J. Chem. Phys.* **1983**, 78, 3494.

(19) Georgiou, K.; Legon, A. C.; Millen, D. J.; Mjoberg, P. J. *Proc. R. Soc. London, A* **1985**, 399, 377.

ESR Study of the Dissociation of Hydroxyl Protons in Hydroxyl Radical Adducts to Pyridinedicarboxylic Acids¹

Hitoshi Taniguchi*

Radiation Laboratory, University of Notre Dame, Notre Dame, Indiana 46556, and Department of Chemistry, Faculty of Liberal Arts, Yamaguchi University, Yamaguchi 753, Japan (Received: April 3, 1987)

The pK_a values for OH proton dissociation in the hydroxyl radical adducts to pyridinedicarboxylic acids have been determined to be 13.0–15.2 in the H_- basicity scale according to in situ radiolysis–steady-state ESR methods. The OH or O⁻ radicals were found to add to ortho and meta positions with respect to a ring nitrogen atom in 2,3-, 3,4-, 3,5-, 2,4-, 2,5-, 2,6-, and 1,4-dihydro-4-oxo-2,6-pyridinedicarboxylic acids. The positions of electron-withdrawing carboxyl groups and a ring nitrogen atom had an effect both upon ESR parameters in acid form and upon pK_a values. Substrate radicals that have a nitrogen atom at the ortho position with respect to the site of OH addition gave larger g values, larger methylenic and ortho proton hyperfine coupling, larger nitrogen hyperfine coupling, and smaller hydroxyl proton hyperfine coupling than those having nitrogen at the meta position. These differences were explained qualitatively. The presence of a ring nitrogen atom affects g factors additively with increments of +0.000 46 and -0.000 19 for ortho and meta substituents, respectively. Remarkable changes in ESR parameters with basicity were found in the dominant methylenic proton and several ring proton and nitrogen hyperfine coupling constants upon the dissociation of the OH proton. The pK_a values are lower by 0.4–1.1 units than corresponding hydroxycyclohexadienyl radicals of benzenedicarboxylic acids, because of an electron-withdrawing character of a ring nitrogen atom. The pK_a values of radicals with carboxyl groups at the ortho position are higher than those of radicals without a carboxyl group at the ortho position, suggesting the existence of specific interactions between the ortho carboxyl and OH or O⁻ groups as is the case in hydroxycyclohexadienyl radicals of carboxylated benzenes.

Introduction

In our previous studies, a basicity scale H_- was established for hydroxycyclohexadienyl radicals,² and it was reported that the pK_a values for the OH proton dissociation in a hydroxymethylene group were determined to be 13.5–15.3 for 13 hydroxycyclohexadienyl radicals from carboxylated benzenes.³

In this paper a detailed in situ radiolysis–ESR study of the dissociation of OH protons has been extended to OH radical adducts to pyridinedicarboxylic acids, in order to find out the electron-withdrawing effect of the ring nitrogen atom. Though the acid form of several OH radical adducts to pyridinedicarboxylic acids was identified already,⁴ acid–base properties of such radicals were not reported yet to the best of our knowledge.

It should be pointed out again that the ESR method has advantages for directly following an acid–base equilibrium of a radical, especially in strongly basic solutions.^{2,3}

Experimental Section

The experimental arrangement and procedures for the observation of OH adduct radicals were essentially the same as those described in the preceding paper.³ All materials were obtained from commercial sources and used without further purification. Sample solutions containing 3–10 mM substrates were saturated with nitrous oxide so that hydrated electron was converted effectively to hydroxyl radical and deoxygenation occurred.³ To provide a basicity scale above the pH scale, our H_- scale² was used for concentrated aqueous potassium hydroxide (KOH) solutions.

(1) The research described herein was supported by the Office of Basic Energy Sciences of the Department of Energy. This is Document No. NDRL-2974 from the Notre Dame Radiation Laboratory. A part of this work was presented at the Sixth International Congress of Radiation Research, Tokyo, May 1979.

(2) Taniguchi, H.; Schuler, R. H. *J. Phys. Chem.* **1985**, 89, 335.

(3) Taniguchi, H.; Schuler, R. H. *J. Phys. Chem.* **1985**, 89, 3095.

(4) Steenken, S.; O'Neill, P. *J. Phys. Chem.* **1978**, 82, 372; *J. Phys. Chem.* **1979**, 83, 2407.

* Address correspondence to this author at the Yamaguchi University.